Terr. Atmos. Ocean. Sci., Vol. 24, No. 4, Part II, 709-719, August 2013 doi: 10.3319/TAO.2013.04.08.01(T)

Multiple Event Analysis of the 2008 M_w 7.9 Wenchuan Earthquake: Implications for Variations in Radiated Seismic Energy During Faulting

Ruey-Der Hwang *

Department of Geology, Chinese Culture University, Taipei, Taiwan

Received 25 October 2012, accepted 8 April 2013

ABSTRACT

A forward modeling of *P*-waves for the 2008 Wenchuan earthquake revealed at least seven sub-events that occurred during faulting with the largest event (i.e., the third sub-event) located at a position ~50 km northeast of the epicenter. Simulations of *P*-waves showed that it would be more appropriate to model the *P*-waves using thrust faulting for the first three sub-events and using strike-slip faulting for the last four. In other words, the faulting for the 2008 Wenchuan earthquake was composed substantially of two mechanisms; the former was a thrust faulting and the latter was a strike-slip rupture. The mechanical transition was near the town of Beichuan, ~100 km northeast of the epicenter. Variations in radiated seismic energy (E_S) showed the largest E_S released from the fourth sub-event. Results also indicated remarkable distinctions between E_S and E_{S0} (called the available energy). On the whole, the total E_S, which was higher than E_{S0} estimated from static stress drop, suggested that the earthquake should be interrupted by a stress model of abrupt-locking. Further, the former thrust faulting released a relatively lower amount of E_S than the latter strike-slip event. Orowan's stress model, i.e., $E_S \approx E_{S0}$, can specify former thrust ruptures implying a high rupture velocity. Because $E_S > E_{S0}$ for latter strike-slip ruptures, a stress model of abrupt-locking, implying higher dynamic stress drop and lower friction during an earthquake, can account for the feature of the latter ruptures. This might suggest that the 2008 Wenchuan earthquake should have a high rupture velocity, perhaps approaching the crustal *S*-wave velocity or even higher.

Key words: Multiple event analysis, Radiated seismic energy, Available energy, Orowan's stress model, Rupture velocity, Dynamic stress drop

Citation: Hwang, R. D., 2013: Multiple event analysis of the 2008 M_w 7.9 Wenchuan earthquake: Implications for variations in radiated seismic energy during faulting. Terr. Atmos. Ocean. Sci., 24, 709-719, doi: 10.3319/TAO.2013.04.08.01(T)

1. INTRODUCTION

The M_w 7.9 Wenchuan earthquake of May 12, 2008 occurred along the Longmenshan fault zone located on the border between the eastern Tibetan plateau and the Sichuan basin (Fig. 1). The earthquake caused extreme destruction in the eastern Sichuan region, China. Aftershocks spread northeastward up to ~300-km occurring to the left of the fault zone to indicate a northwest-dipping fault plane (Fig. 1). Analysis of rupture directivity from surface waves also showed a northeastward rupture with an azimuth of N59°E (Hwang et al. 2011). Field surveys identified an obvious surface rupture terminating near the town of Shikan (also see Fig. 1) (Liu-Zeng et al. 2009; Xu et al. 2009a). Ji and Hayes (2008) and Nishimura and Yagi (2008) first reported source rupture models for the 2008 Wenchuan earthquake from body-wave inversions and was comparable with others (e.g., Hashimoto et al. 2010; Nakamura et al. 2010). Variations in rupture velocity with an average of 2.6 - 2.9 km s^{-1} were also documented in Wen et al. (2012). These source models not only exhibited the complexity of the earthquake, but also indicated that the rupture mechanism varied from thrust faulting to strike-slip faulting along the fault. Nakamura et al. (2010) further stated that the transformation of faulting mechanisms occurred ~110 km northeast of the epicenter. Additionally, slip distributions estimated from GPS and InSAR data revealed larger slips near the towns of Yingxiu, Beichuan, and Nanba (Hao et al. 2009; Shen et al. 2009; Xu et al. 2009b).

Investigation of the 2008 Wenchuan earthquake from seismic and GPS data focus primarily on understanding

* *Corresponding author*
E-mail: hrd@faculty.pccu.edu.tw

source rupture features. However, macroscopic source parameters (as radiated seismic energy) are also useful to grasp the rupture features of earthquakes (Kikuchi and Fukao 1988; Kanamori 1994; Kanamori and Heaton 2000). In general, radiated seismic energy can either be determined from the integration of seismic waves (e.g., Choy and Boatwright 1995; Hwang et al. 2001; Pérez-Campos and Beroza 2001) or source time function (e.g., Vassiliou and Kanamori 1982; Kikuchi and Fukao 1988; Hwang et al. 2010, 2012; Hwang 2012). Scaled energy, the ratio (E_S/M_0) of radiated seismic energy (E_S) to seismic moment (M_0), is related to the dynamics of earthquake faulting. A rapid drop in friction during earthquake faulting results in a large E_S/M_0, whereas a slower drop in friction leads to a relatively low E_S/M_0 (Kanamori and Heaton 2000). However, uncertainty in the estimated radiated seismic energy would cause high divergence in the ratio of E_S/M_0 (Kanamori 1994; Kanamori and Heaton 2000). Furthermore, the usage of a finite frequency

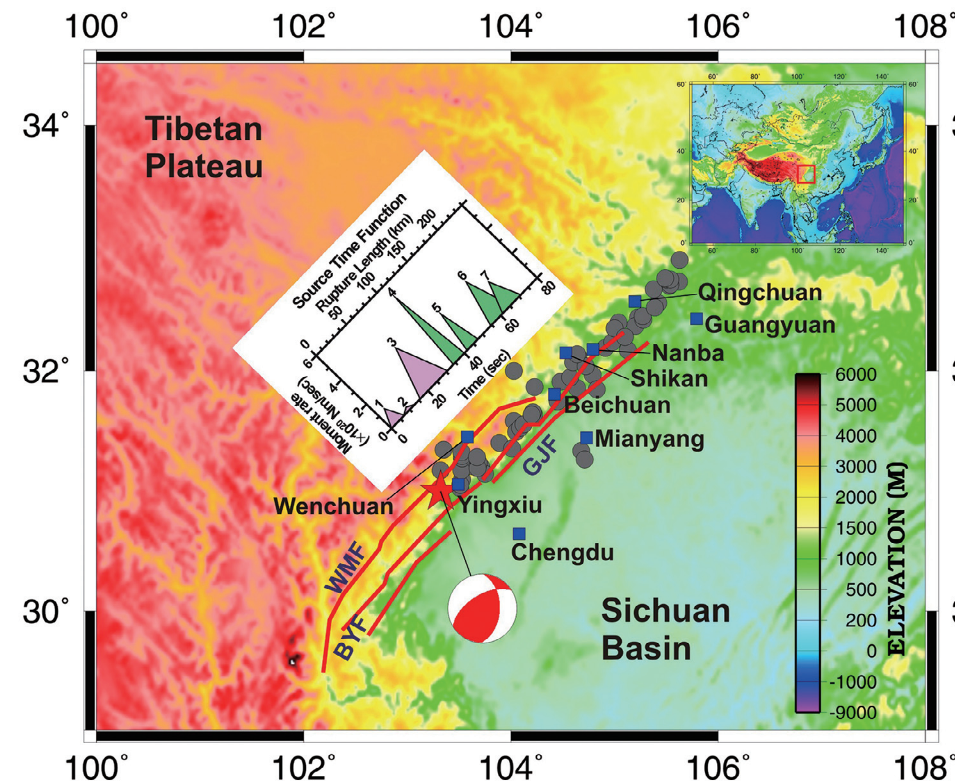

Fig. 1. Maps showing the topography (data from NGDC, National Geophysical Data Center) around the source area of the 2008 Wenchuan earthquake. The star and circles denote the main shock and aftershocks (mb ≥ 5.0). The beach ball stands for the focal mechanism reported by the USGS. The closed squares indicate several cities around the source area. Three faults displayed by red lines in the Longmenshan fault zone are Wenchuan-Maowen fault (WMF), Beichuan-Yingxiu fault (BYF) and Guanxian-Jiangyou fault (GJF). Source time function is also included: numbers 1 - 3 for the sub-events with thrust faulting and numbers 4 - 7 for the sub-events with strike-slip faulting as in Table 1.

Table 1. Source parameters derived in this study.

No.	Focal mechanism (strike/dip/rake)	Source duration (sec)	Time to the first sub-event (sec)	Seismic moment ($\times 10^{20}$ Nm)	E_S ($\times 10^{16}$ Nm)	M_w
1	231°/35°/138°	7.0	0.0	0.380	0.213	7.0
2	231°/35°/138°	6.0	6.7	0.076	0.014	6.5
3	231°/35°/148°	15.0	15.7	2.280	0.780	7.5
4	231°/35°/181°	6.0	34.0	1.520	5.420	7.4
5	231°/55°/195°	6.0	41.5	0.760	1.354	7.2
6	231°/55°/195°	11.0	54.5	1.520	0.879	7.4
7	231°/55°/195°	10.0	61.0	0.912	0.421	7.2

Note: (1) Total seismic moment = 7.448×10^{20} Nm (M_w = 7.85). (2) Total E_S = 9.081×10^{16} Nm.

bandwidth in seismic waves would also give rise to an underestimation of E_S, due to a lack of high-frequency content (e.g., Wang 2004). The estimation of E_S from the source time functions of multiple events (Kikuchi and Fukao 1988; Hwang et al. 2008; Hwang 2012) and finite-fault source model (Kanamori 2006) appears to detect a certain amount of high-frequency energy. In spite of the difficulties in estimating radiated seismic energy, the E_S/M_0 of strike-slip earthquakes is significantly different from that of reverse or normal earthquakes (e.g., Choy and Boatwright 1995; Pérez-Campos and Beroza 2001). Hence, to gain a deeper understanding in the rupture behavior of the 2008 Wenchuan earthquake, the purpose of this study is to investigate the multiple shocks through forward *P*-waves modeling and subsequently estimate the E_S of each sub-event to state the dynamic rupture process during the earthquake from the viewpoint of macroscopic source parameters.

2. DATA

During the 2008 Wenchuan earthquake, the Incorporated Research Institutions for Seismology Data Management Center (IRIS DMC) collected hundreds of seismograms, recorded by global seismic networks. This provided a wealth of high-quality seismic data from which it is of great use to analyze the rupture feature of the 2008 Wenchuan earthquake. To avoid interference from core phases (such as *PcP*-waves) or multipath waves (such as *PP*-waves) on the direct *P*-waves, this study only used *P*-waves from the vertical-component seismograms recorded at epicentral distances of 30° - 90°. From an empirical relationship between seismic moment and source duration (Furumoto and Nakanishi 1983), the 2008 Wenchuan earthquake had a source duration of ~70 sec estimated from the seismic moment of 7.6×10^{20} Nm as reported by the US Geological Survey (USGS). Taking account of the effects of rupture directivity to the 2008 Wenchuan earthquake, we extracted a 145-sec-long seismogram, including the first 5 sec of the *P*-arrival and continuing for 140 sec after the *P*-arrival. Figure 2a shows the available stations around the epicenter.

3. FOCAL DEPTHS FOR SUB-EVENTS

In Fig. 2b, the seismograms generated by the 2008 Wenchuan earthquake showed obvious multiple sources as observed at station ESK, particularly for the first 50 sec of recordings. The first *P*-arrival was the first sub-event, and the maximum sub-event appeared ~16-sec after the first *P*-arrival. We inverted the focal depths of the two sub-events from the extracted waveforms as shown in Fig. 2b by a teleseismic *P*-wave inversion method of Lin et al. (2008) (also refer to Hwang et al. 2012). The 2008 Wenchuan earthquake was a shallow source such that the synthetic *P*-waves must include two depth phases (*pP*- and *sP*-waves), excluding the direct *P*-wave (cf. Lin et al. 2006; Hwang et al. 2010, 2012). The *P*-waves were created synthetically following the *iasp91* velocity model (Kennett and Engdahl 1991) (also see Appendix A). In the analysis, the *PP*-wave would probably influence the *P*-waves. For a shallow source depth, the *PP*-wave arrived at ~68 sec after the onset for an epicentral distance of 30° and at ~212 sec after the onset for an epicentral distance of 90°. Since the two sub-events were within the first 50 sec of recordings, the *PP*-wave would not interfere with the two sub-events. Figure 2c shows the

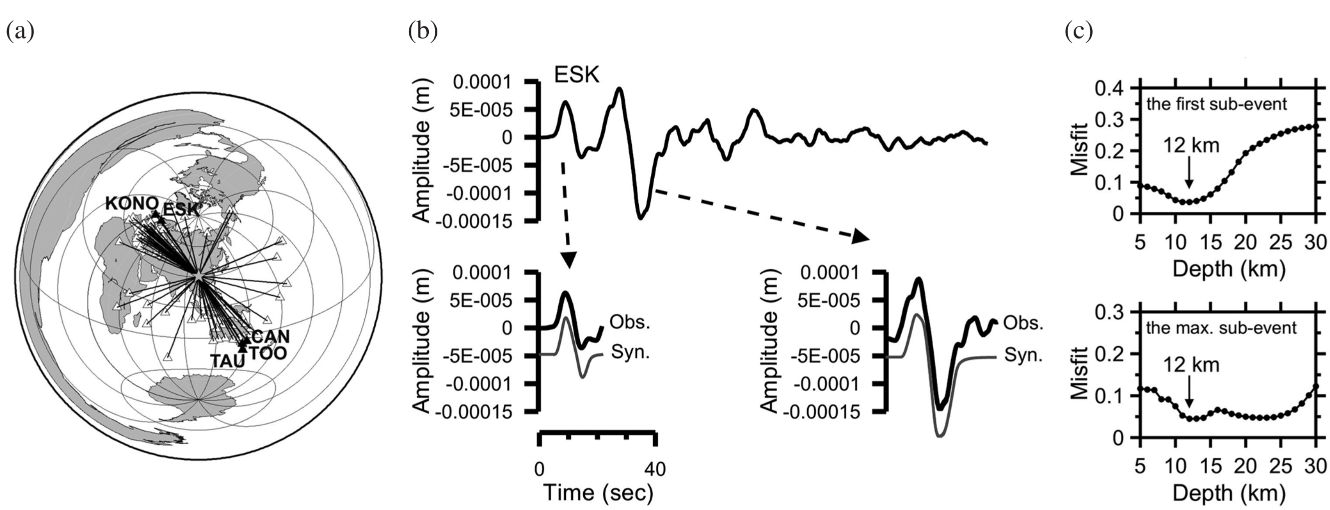

Fig. 2. (a) Stations (open triangles) used to determine the focal depth of two sub-events. The closed triangles are the stations, ESK, KONO, CAN, TAU and TOO, independent of the source rupture directivity and used to investigate the multiple sources. (b) Seismogram (*P*-waves) at station ESK shows two obvious sub-events. The gray lines denote the synthetic *P*-waves and the black lines are the observed *P*-waves. (c) Misfit between the observed and synthetic *P*-waves indicates the best focal depth ~12 km for the two sub-events in (b).

misfit between observed and synthetic *P*-waves for the two sub-events and indicates an ideal focal depth of 12 km.

4. MULTIPLE EVENT ANALYSIS AND RADIATED SEISMIC ENERGY

As mentioned above, the two sub-events (Fig. 2) had a focal depth of 12 km. Aftershocks occurred mainly within depths of 20 km and were distributed from southwest to northeast (Fig. 1). An analysis of surface waves indicated the optimal rupture direction of N59°E which agrees with the distribution of aftershocks (Hwang et al. 2011). Here we assumed that all sub-events occurred at a focal depth of 12 km and successively ruptured the Longmenshan fault zone from the epicenter toward N59°E. For simplification in the forward *P*-wave modeling only stations located at the azimuth normal to the rupture direction of the 2008 Wenchuan earthquake were used to perform the multiple-event analysis. Therefore, from the geometry of the ray-path to the direction of rupture, several stations, KONO, ESK, CAN, TOO and TAU as in Fig. 2a, were considered to be independent of rupture directivity and appropriate for the multiple-event analysis. The epicentral distances of the stations employed for the multiple event analysis were 65° - 85°; hence, the *PP*-wave arrived at ~140 - 195 sec after the first *P*-arrival. That is, the *PP*-wave would not interfere with the *P*-wave modeling in this study. Furthermore, these stations used for the multiple event analysis had take-off angles of 15 - 20 degrees; thus, all located on the compression quadrant from which the *P*-waves have an upward first-motion (i.e., positive polarization). In addition, the phases (*PmPP*, *pPmp*, and *PPmp* etc.) from the Moho reflection near the source and receiver are also discounted in waveform modeling because of their small amplitudes compared with the initial *P*-waves through the calculations of reflection coefficients.

In this study, the synthetic *P*-wave train (i.e., direct *P*-wave, *pP*- and *sP*-waves) for forward modeling was calculated according to a point source with a triangular source time function and the *iasp91* model (cf. Lin et al. 2006; Hwang et al. 2010, 2012; also see Appendix A). Before the multiple-event analysis using the forward modeling of *P*-waves, we used an empirical Green's function (EGF) deconvolution technique to investigate roughly the multiple sources of the 2008 Wenchuan earthquake. First, the synthetic *P*-waves (Fig. 3), as the EGFs (Ammon et al. 2006), were produced at stations CAN and ESK using a delta source time function, a source depth of 12 km, and a thrust fault plane of 231°/35°/138° (strike/dip/rake). In Fig. 3, the retrieved relative source time function (RSTF) showed several obvious sub-events. The largest sub-event with source duration of ~17 sec was about 16 sec later after the onset (i.e., the first sub-event with source duration of ~5 - 8 sec). The initial feature was in agreement with the work of Wen et al. (2012). In addition, the largest sub-event was followed by two sub-events, ~35 and ~45 sec later after the onset, respectively. From Fig. 3, roughly speaking, five obvious sub-events occurred during the earthquake. However, from waveform readings, it seemed to have two extra sub-events occurring after ~45 sec. With regard to waveforms appear-

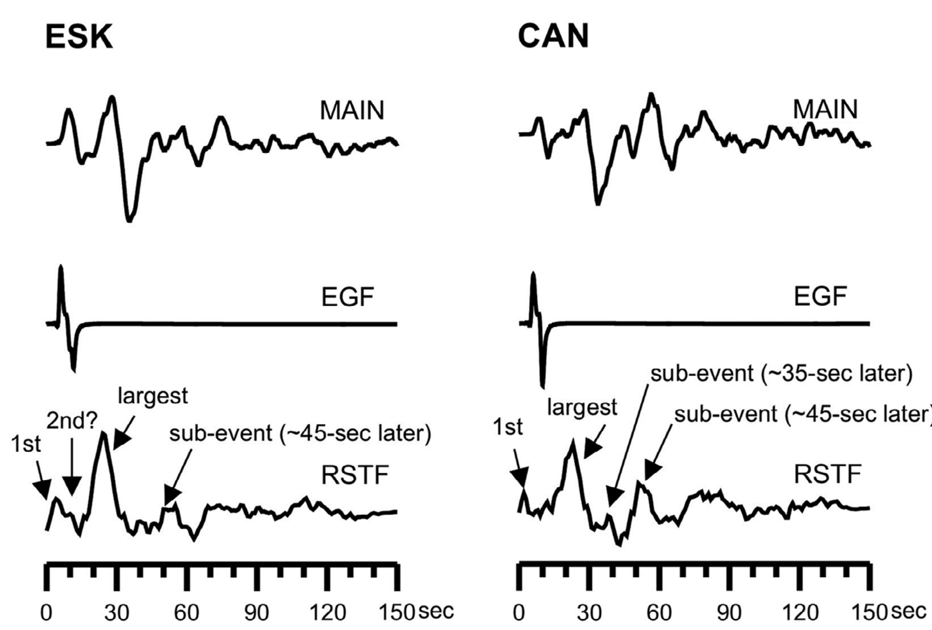

Fig. 3. Using an empirical Green's function (EGF) deconvolution technique to retrieve the relative source time function (RSTF), revealing roughly the feature of multiple sources for the 2008 Wenchuan earthquake. The EGFs were created synthetically at stations CAN and E_SK using a delta source time function, a source depth of 12 km, and a thrust fault plane of 231°/35°/138° (strike/dip/rake).

ing after ~70 sec, it cannot be confirmed if the signals were released from the earthquake rupture. For this reason, the purpose of this study was only to analyze seven sub-events during the 2008 Wenchuan earthquake up to ~70 sec, and to calculate the radiated seismic energy for each sub-event. Subsequently, we modulated the time lag relative to the first sub-event, source duration and seismic moment for each sub-event to ensure that the synthetic *P*-waves corresponded with the observed *P*-waves. This analysis was a process of trial and error. Recordings in stations CAN and ESK were taken as examples to interpret the procedure of multiple-event analysis as displayed in Fig. 4.

In this study, we modeled the *P*-waves for each sub-event under fixing the strike of fault plane (231°). In Fig. 4a, it was necessary to add a sub-event between the first and the largest sub-events for a better waveform fitting. Then again, the first three sub-events can be modeled well using a thrust mechanism wherein the status is from the GCMT's report (see Table 1). To put the fourth sub-event (~35-sec later to the onset) using a thrust (231°/35°/138°) or a strike-slip (231°/35°/181°) mechanism to model the *P*-waves showed that the synthetic waveforms seemed to match the observed waveforms in Figs. 4b and c. However, using a thrust faulting to the fourth sub-event would underestimate the seismic moment of this sub-event. When using thrust mechanisms (231°/35°/138°) to model all sub-events, the synthetic waveforms were out of phase compared with the observations (shown in Fig. 4d). Such waveform modeling resulted in a lower seismic moment for the earthquake. That is, the mechanisms of sub-events after the largest sub-event must be different from the first three sub-events. Figure 4e shows that the rest of the sub-events after the largest sub-event were modeled using a strike-slip mechanism of 231°/35°/181°, but the fitting between the observed and synthetic *P*-waves was not perfect and the seismic moment was overestimated. As a result, a change in the status of the strike-slip faulting is necessary for the last three sub-events. During testing, the dip and rake in the last three sub-events had to be changed slightly to obtain a better fit between the observed and synthetic *P*-waves as shown in Table 1 and Fig. 4f. To model *P*-wave for the fourth sub-event using a mechanism of 231°/55°/195°, similar to the last three sub-events, would

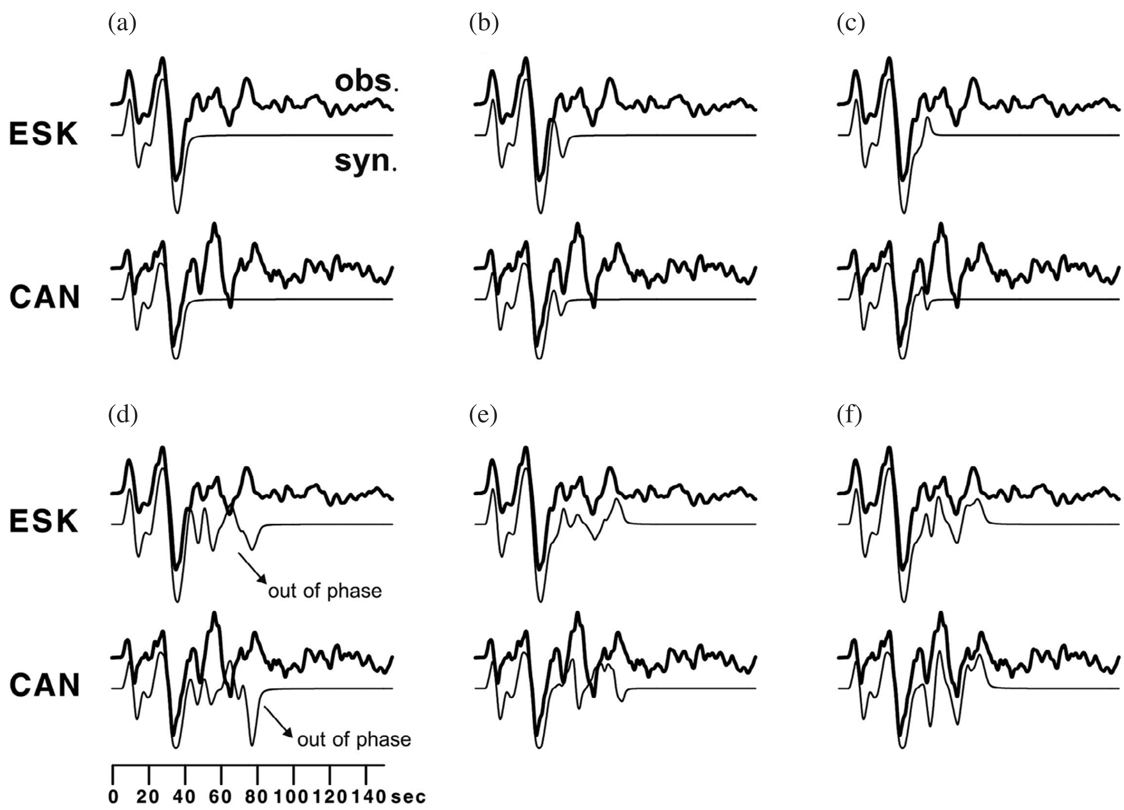

Fig. 4. *P*-waves observed at stations CAN and ESK are taken as examples to account for the procedure of multiple-event analysis. The thick lines denote the observed *P*-waves and the thin lines stand for the synthetic ones. (a) The first three sub-events modeled using a thrust mechanism as in Table 1. (b) and (c) The fourth sub-event modeled by a thrust and a strike-slip faulting, respectively. (d) The *P*-waves modeled using a thrust mechanism to all sub-events. The synthetic *P*-waves show out of phase relative to the observed *P*-waves after ~35 sec. (e) The first three sub-events modeled using a thrust mechanism and the last four sub-events modeled using a strike-slip mechanism. (f) The synthetic *P*-waves modeled using a slight change in the mechanisms for the last three sub-events show a better fitting as compared with the observed *P*-waves. For details in the multiple event analysis based on trial and error, refer to the text.

also lead to an underestimation of seismic moment. Because we could not confirm whether the later phases after 70 sec from the first *P*-arrival were generated by the source rupture, we conservatively estimated the source duration to be 71 sec (Table 1).

As mentioned above, results by the forward test based upon trial and error showed that the 2008 Wenchuan earthquake consisted of at least seven sub-events during the rupture (Table 1 and Fig. 5). We deemed it better to fit observed *P*-waves using thrust faulting for the first three sub-events and strike-slip faulting for the last four sub-events (Fig. 4). Additionally, the fault status used to compute the synthetic *P*-waves for the last four sub-events in the northern segment of the fault had a greater dip angle (55°) relative to the first three sub-events (35°) in the southern segment. With this analysis, the total source duration and seismic moment were 71 sec and 7.448×10^{20} Nm ($M_w = 7.85$), respectively. Table 1 lists the preferred multiple-source parameters for each sub-event, including seismic moment, source duration, and time of occurrence to the first sub-event.

Vassiliou and Kanamori (1982) proposed a method to calculate the E_S using source duration (also see Appendix A). By taking the *P*-wave of 5.8 km s^{-1}, *S*-wave of 3.36 km s^{-1} and density of 2.45 g cm^{-3} in the source area, the estimated E_S for the seven sub-events varied along the fault from 0.014×10^{16} Nm to 5.420×10^{16} Nm with the maximum intensity measured at the fourth sub-event; the total E_S was 9.081×10^{16} Nm. Table 1 also lists the E_S for each sub-event.

5. DISCUSSION

The multiple event analysis indicates that at least seven sub-events occurred during the 2008 Wenchuan earthquake rupturing the Longmenshen fault zone (Figs. 1, 4, and 5). The third sub-event has the largest seismic moment (corresponding to $M_w = 7.5$) located at a position ~50 km NE from the epicenter (Fig. 1). The largest sub-event dominates the entire rupture mechanism as thrust faulting, as reported by the USGS and GCMT (Global CMT). From Table 1, the largest sub-event started at 15.7 sec and stopped at 30.7 sec with the peak energy at 23.2 sec and source duration of 15 sec. Hence, the maximum energy release occurs around 20 - 30 sec from this study, also consistent with those from previous studies (e.g., Wang et al. 2008; Nakamura et al. 2010; Wen et al. 2012). Application of the thrust mechanism to all sub-events during analysis leads to a failure in waveform fitting between the observed and synthetic *P*-waves, whereas using the thrust mechanism for the first three sub-events and the strike-slip mechanism for the last four sub-events provides a better waveform fitting (Table 1 and Figs. 4 - 5). That is, the source rupture for the 2008 Wenchuan earthquake can be divided into two faulting mechanisms; the former is a thrust faulting and the latter is a strike-slip one (cf. Ji and Hayes 2008; Nishimura and Yagi 2008; Hao et al.

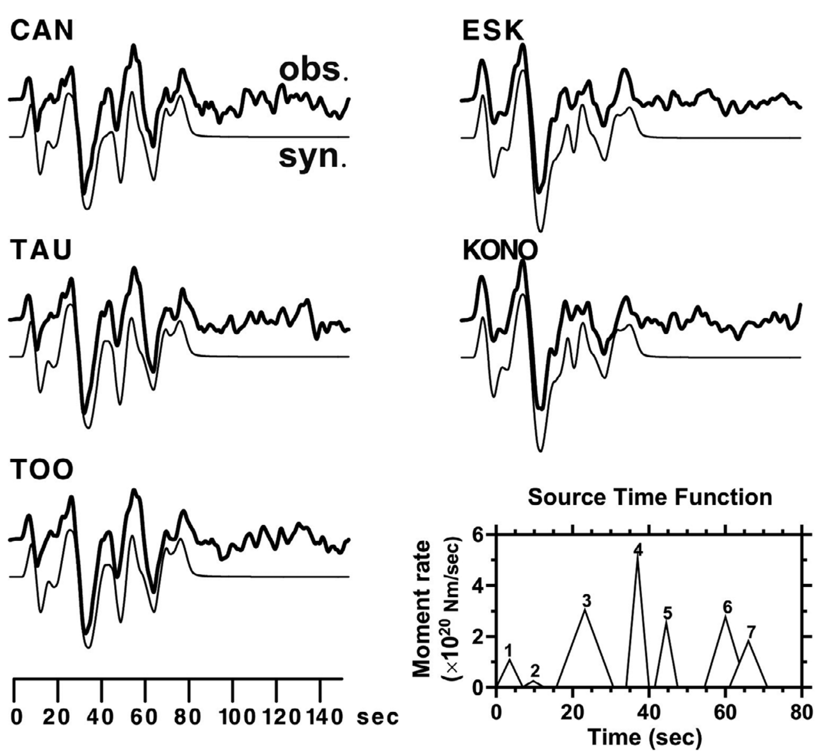

Fig. 5. Comparisons of the observed (thick lines) and synthetic (thin lines) *P*-waves at several stations, located at azimuths normal to the rupture direction. The source time function for the seven sub-events from the forward *P*-waves modeling is also shown.

2009; Shen et al. 2009; Hashimoto et al. 2010; Nakamura et al. 2010; Wen et al. 2012). In addition, the last three sub-events with strike-slip faulting required a larger dip angle (~55°), compared with those with the thrust faulting (cf. Shen et al. 2009; Xu et al. 2009a). Table 1 shows the latter strike-slip ruptures with slightly normal faulting, which are different from the previous source rupture models (e.g., Wang et al. 2008; Shen et al. 2009; Nakamura et al. 2010). However, such results from this study seem comparable with those from Zhang et al. (2009).

In Table 1, the time difference, ~18 sec, between the third and fourth sub-events appears to show that the ruptures are obstructed in a region, where the fault status is variable (Shen et al. 2009). The transition in mechanism from thrust to strike-slip faulting occurs ~34.0 sec later after the onset and is ~100 km NE of the epicenter using an average rupture velocity of 3.0 km s^{-1} (Hwang et al. 2011; Hartzell et al. 2013). The location of mechanism transformation is near the town of Beichuan (Fig. 1), where field surveys also denoted the change in fault status (Liu-Zeng et al. 2009; Xu et al. 2009a). The multiple-event analysis from this study is also comparable with the work of Wen et al. (2012), using the EGF deconvolution to reveal the time in change of faulting mechanism is ~35 sec.

By adopting an average rupture velocity ~3.0 km s^{-1} derived from the rupture directivity analysis of surface waves (Hwang et al. 2011) or the source rupture model used by Hartzell et al. (2013), we derived a rupture length of approximately 210 km for the 2008 Wenchuan earthquake. The rupture length derived from this study is the so-called effective length which was created by the main energy release during earthquake rupture. Generally speaking, the effective rupture length is shorter than the surface rupture length (cf. Yen and Ma 2011). According to Mai and Beroza (2000), the effective rupture length for the 2008 Wenchuan earthquake is ~240-km-long from the source model of Ji and Hayes (2008), and ~190-km-long from that of Sladen (2008). From field investigation, the surface rupture length is ~240 km from Xu et al. (2009a), ~240 km from Zhou et al. (2010), ~230 km from Liu-Zeng et al. (2009), and ~285 km from Lin et al. (2009). Xu et al. (2009b) using a *P*-wave back-projection also indicated that there is a relatively low energy release (< 30% of total energy releases) to the town of Qingchuan (see Fig. 1) implying the effective rupture length to be shorter than 250 km. Because we were unable to confirm whether or not the waves arriving at 70 sec after the first *P*-arrival as those in Fig. 2b were signals released from the main shock, this study only estimates the source duration to be 71 sec. Although the estimated rupture length and source duration are shorter than those derived from several source rupture models (e.g., Ji and Hayes 2008; Nishimura and Yagi 2008; Hao et al. 2009; Shen et al. 2009; Hashimoto et al. 2010; Nakamura et al. 2010; Wen et al. 2012) and field surveys of surface ruptures (Lin et al. 2009; Liu-Zeng et al. 2009; Xu et al. 2009a; Zhou et al. 2010), this study is comparable to those from rupture directivity analysis of surface waves (Hwang et al. 2011) and a source rupture model of Sladen (2008). An empirical relationship between the seismic moment and source duration (Furumoto and Nakanishi 1983) suggests that the 2008 Wenchuan earthquake should have a source duration of ~67 sec from $M_0 = 7.448 \times 10^{20}$ Nm (this study), ~71 sec from $M_0 = 8.97 \times 10^{20}$ Nm (GCMT), and ~73 - 76 sec from $M_0 = 1.0 - 1.1 \times 10^{21}$ Nm (Wen et al. 2012; Harztell et al. 2013). In terms of the effective rupture length and source duration, the results from this study seem acceptable.

Following Vassiliou and Kanamori (1982), the total E_S is 9.081×10^{16} Nm and the fourth sub-event has the maximum E_S ~5.420×10^{16} Nm (Table 1). The estimated E_S is greater than that derived from the USGS (1.4×10^{16} Nm) and surface-wave analysis (5.93×10^{16} Nm) (Hwang et al. 2011), but these results still have the same order of magnitude. The lower E_S from the surface-wave analysis is because the surface-wave analysis used a single source model to result in an underestimation in E_S. The multiple-event analysis reveals more E_S during earthquake rupture than from the surface-wave analysis. Such multiple event analysis (Kikuchi and Fukao 1988; Hwang et al. 2008, Hwang 2012) seems to decrease the effect of finite-frequency bandwidth on the estimate of E_S (Wang 2004). Overall, the E_S/M_0 ratio ~1.22×10^{-4} for the Wenchuan earthquake is larger than those (5×10^{-5}) for ordinary earthquakes, and then a rapid drop in friction may occur during earthquake faulting which implies a high rupture velocity (e.g., Kanamori and Heaton 2000).

Since the rupture process includes two faulting mechanisms from the forward multiple event analysis, here we divide the ruptures into two parts. The first part is a thrust rupture (i.e., the first three sub-events) with the radiated seismic energy (E_{ST}) of 1.007×10^{16} Nm; the other (i.e., the last four sub-events) is a strike-slip rupture with the radiated seismic energy (E_{SS}) of 8.074×10^{16} Nm. In the Orowan model, in which the dynamic stress equals the final stress during faulting (cf. Kanamori 1994), the radiated seismic energy can be expressed as $E_{S0} = (M_0 \Delta\sigma)/(2\mu)$, where $\Delta\sigma$ is the static stress drop, M_0 is the seismic moment and μ is rigidity. The E_{S0} is referred to as available energy estimated from $\Delta\sigma$ and M_0 (cf. Kanamori and Rivera 2006). Kanamori (1994) summarized the stress models to account for the dynamic ruptures during the earthquakes. For an Orowan fault model, then E_S equals E_{S0}; for a stress model of frictional overshoot, then E_S is smaller than E_{S0}; for an abrupt-locking stress model, then E_S is larger than E_{S0}. Broadly speaking, the 2008 Wenchuan earthquake exhibits slips coinciding with an abrupt-locking stress model, because the total E_S (9.081×10^{16} Nm) estimated in this study was larger than E_{S0} (4.475×10^{16} Nm) calculated from the static stress drop of ~32.5 bars following Hwang et al. (2011).

The effective rupture length for the thrust faulting is ~102 and ~111 km for the strike-slip faulting using an average rupture velocity of 3.0 km s^{-1} (Table 1). The efficient width of the fault for the Wenchuan earthquake is about 30.8 km estimated from the source model provided by Ji and Hayes (2008). According to a rectangular finite-fault model with surface rupture (Kanamori and Anderson 1975), for the ruptures with thrust faulting $\Delta\sigma$ is ~24 bars estimated from the fault length ~102 km and fault width ~30.8 km; for the ruptures with strike-slip faulting $\Delta\sigma$ is ~28.5 bars calculated from the fault length ~111 km and fault width ~30.8 km. For the thrust faulting, the available energy (E_{ST0}) is 1.190×10^{16} Nm, calculated from $\Delta\sigma = 24$ bars and $M_0 = 2.736 \times 10^{20}$ Nm, and approximates to E_{ST} of 1.007×10^{16} Nm; for the strike-slip faulting, the available energy (E_{SS0}) is 2.433×10^{16} Nm, derived from $\Delta\sigma = 28.5$ bars and $M_0 = 4.712 \times 10^{20}$ Nm, and lower than E_{SS} of 8.074×10^{16} Nm. As a result, the Orowan model is likely to describe the rupture behavior of the former thrust faulting due to $E_{ST} \approx E_{ST0}$, in which high rupture velocity occurs. The rupture feature of the last strike-slip faulting corresponds to an abrupt-locking stress model because of $E_{SS} > E_{SS0}$, indicating a higher dynamic stress drop and low friction during faulting (Kanamori 1994; Kanamori and Heaton 2000). The E_S/M_0 ratio (3.68×10^{-5}) for the former thrust rupture is also significantly lower than that (1.71×10^{-4}) for the last strike-slip rupture. The feature also agrees with global observations, from which the strike-slip earthquakes have relatively larger E_S/M_0 (e.g., Choy and Boatwright 1995; Pérez-Campos and Beroza 2001).

6. CONCLUSIONS

Multiple event analysis from the forward *P*-wave modeling exhibited the complexity of ruptures during the 2008 Wenchuan earthquake. The rupture process demonstrated two main faulting mechanisms: first, there was a thrust mechanism for the first three sub-events and the other was a strike-slip mechanism for the last four sub-events. The transition position of the faulting mechanism seemed to be near Beichuan town, ~100-km northeast of the epicenter (Fig. 1). The mechanism transformation might be related to changes in fault status, particularly for variations in the dip-angle of the fault as it increased along the fault from southwest to northeast (Shen et al. 2009; Xu et al. 2009a). From a view of a single source, the Wenchuan earthquake can be interrupted by a stress model of abrupt-locking due to $E_S > E_{S0}$. In terms of the variations in E_S and E_{S0} for the multiple sources, the dynamic ruptures varied from Orowan's stress model to abrupt-locking stress processes during the Wenchuan earthquake. Such results also implied a high rupture velocity for the 2008 Wenchuan earthquake. Through multiple event analysis, this study not only revealed the complexity of the rupture, but also provided a deeper understanding of dynamic process involved in the ruptures during the 2008 Wenchuan earthquake.

Acknowledgements I thank the two anonymous reviewers for their critical suggestions to improve the manuscript. Here I would like to express our gratitude to the IRIS (Incorporated Research Institutes for Seismology) for providing us with the Global Seismic Network (GSN) data. The National Science Council, ROC (No. NSC101-2116-M-034-002-MY2) supported partly the finances for this study.

REFERENCES

Aki, K. and P. G. Richards, 2002: Quantitative Seismology, 2nd Ed., University Science Books, Sausalito, CA, 700 pp.

Ammon, C. J., A. A. Velasco, and T. Lay, 2006: Rapid estimation of first-order rupture characteristics for large earthquakes using surface waves: 2004 Sumatra-Andaman earthquake. *Geophys. Res. Lett.*, **33**, L14314, doi: 10.1029/2006GL026303. [Link]

Choy, G. L. and J. L. Boatwright, 1995: Global patterns of radiated seismic energy and apparent stress. *J. Geophys. Res.*, **100**, 18205-18228, doi: 10.1029/95JB01969. [Link]

Furumoto, M. and I. Nakanishi, 1983: Source times and scaling relations of large earthquakes. *J. Geophys. Res.*, **88**, 2191-2198, doi: 10.1029/JB088iB03p02191. [Link]

Hao, K. X., H. Si, H. Fujiwara, and T. Ozawa, 2009: Coseismic surface-ruptures and crustal deformations of the 2008 Wenchuan earthquake *Mw*7.9, China. *Geophys. Res. Lett.*, **36**, L11303, doi: 10.1029/2009GL037971. [Link]

Hartzell, S., C. Mendoza, L. Ramirez-Guzman, Y. Zeng, and W. Mooney, 2013: Rupture history of the 2008 M_w 7.9 Wenchuan, China, earthquake: Evaluation of separate and joint inversions of geodetic, teleseismic, and strong-Motion data. *Bull. Seismol. Soc. Am.*, **103**, 353-370, doi: 10.1785/0120120108. [Link]

Hashimoto, M., M. Enomoto, and Y. Fukushima, 2010: Coseismic deformation from the 2008 Wenchuan, China, earthquake derived from ALOS/PALSAR images. *Tectonophysics*, **491**, 59-71, doi: 10.1016/j.tecto.2009.08.034. [Link]

Hwang, R. D., 2012: Estimating the radiated seismic energy of the 2010 M_L 6.4 JiaSian, Taiwan, earthquake using multiple-event analysis. *Terr. Atmos. Ocean. Sci.*, **23**, 459-465, doi: 10.3319/TAO.2012.03.30.01(T). [Link]

Hwang, R. D., J. H. Wang, B. S. Huang, K. C. Chen, W. G. Huang, T. M. Chang, H. C. Chiu and C.-C. P. Tsai, 2001: Estimates of stress drop of the Chi-Chi, Taiwan, earthquake of 20 September 1999 from near-field seismograms. *Bull. Seismol. Soc. Am.*, **91**, 1158-1166, doi: 10.1785/0120000708. [Link]

Hwang, R. D., G. K. Yu, T. W. Lin, J. P. Chang, and W. Y. Chang, 2008: Radiated seismic energy of 26 December 2004 Sumatra earthquake estimated from multiple-event analysis. Annual Congress of Chinese Geophysical Society and Geological Society of Taiwan, Tainan, Taiwan, May 7 - 8, 2008. (in Chinese)

Hwang, R. D., T. W. Lin, G. K. Yu, J. P. Chang, and W. Y. Chang, 2010: Source parameters of the 2005 M_w 7.2 Miyagi-Oki, Japan, earthquake as inferred from teleseismic *P*-waves. *Terr. Atmos. Ocean. Sci.*, **21**, 645-654, doi: 10.3319/TAO.2009.08.25.01(T). [Link]

Hwang, R. D., J. P. Chang, C. Y. Wang, J. J. Wu, C. H. Kuo, Y. W. Tsai, W. Y. Chang, and T. W. Lin, 2011: Rise time and source duration of the 2008 M_w 7.9 Wenchuan (China) earthquake as revealed by Rayleigh-waves. *Earth Planets Space*, **63**, 427-434, doi: 10.5047/eps.2011.01.002. [Link]

Hwang, R. D., T. W. Lin, C. C. Wu, W. Y. Chang, and J. P. Chang, 2012: Reexamining the source parameters of the 2010 M_L 6.4 JiaSian (Taiwan) earthquake using the inversion of teleseismic *P*-waves. *J. Asian Earth Sci.*, **48**, 24-30, doi: 10.1016/j.jseaes.2011.12.021. [Link]

Ji, C. and G. Hayes, 2008: Preliminary result of the May 12, 2008 M_w 7.9 Eastern Sichuan, China Earthquake. Available at http://earthquake.usgs.gov/eqcenter/eqinthenews/2008/us2008ryan/finite_fault.php.

Kanamori, H., 1994: Mechanics of earthquakes. *Annu. Rev. Earth Planet. Sci.*, **22**, 207-237, doi: 10.1146/annurev.ea.22.050194.001231. [Link]

Kanamori, H., 2006: The radiated energy of the 2004 Sumatra-Andaman earthquake. In: Abercrombie, R., A. McGarr, H. Kanamori, and G. Di Toro (Eds.), Earthquake: Radiated Energy and the Physics of Faulting, Geophysical Monograph Series, vol. 170, American Geophysical Union, Washington, DC, 327 pp, doi: 10.1029/GM170. [Link]

Kanamori, H. and D. L. Anderson, 1975: Theoretical basis of some empirical relations in seismology. *Bull. Seismol. Soc. Am.*, **65**, 1073-1095.

Kanamori, H. and G. Stewart, 1976: Mode of the strain release along the Gibbs fracture zone, Mid-Atlantic ridge. *Phys. Earth Planet. Inter.*, **11**, 312-332, doi: 10.1016/0031-9201(76)90018-2. [Link]

Kanamori, H. and T. H. Heaton, 2000: Microscopic and macroscopic physics of earthquakes. In: Rundle, J. B., D. L. Turcotte, and W. Klein (Eds.), Geocomplexity and the Physics of Earthquakes, Geophysical Monograph Series, vol. 120, American Geophysical Union, Washington, DC, 284 pp, doi: 10.1029/GM120. [Link]

Kanamori, H. and L. Rivera, 2006: Energy partitioning during an earthquake. In: Abercrombie, R., A. McGarr, H. Kanamori, and G. Di Toro (Eds.), Earthquake: Radiated Energy and the Physics of Faulting, Geophysical Monograph Series, vol. 170, American Geophysical Union, Washington, DC, 327 pp, doi: 10.1029/GM170. [Link]

Kennett, B. L. N. and E. R. Engdahl, 1991: Traveltimes for global earthquake location and phase identification. *Geophys. J. Int.*, **105**, 429-465, doi: 10.1111/j.1365-246X.1991.tb06724.x. [Link]

Kikuchi, M. and Y. Fukao, 1988: Seismic wave energy inferred from long-period body wave inversion. *Bull. Seismol. Soc. Am.*, **78**, 1707-1724.

Lin, A., Z. Ren, D. Jia, and X. Wu, 2009: Co-seismic thrusting rupture and slip distribution produced by the 2008 M_W 7.9 Wenchuan earthquake, China. *Tectonophysics*, **471**, 203-215, doi: 10.1016/j.tecto.2009.02.014. [Link]

Lin, T. W., R. D. Hwang, K. F. Ma, and Y. B. Tsai, 2006: Simultaneous determination of earthquake source parameters using far-field P waves: Focal mechanism, seismic moment, rupture length and rupture velocity. *Terr. Atmos. Ocean. Sci.*, **17**, 463-487.

Lin, T. W., R. D. Hwang, J. P. Chang, G. K. Yu, and W. Y. Chang, 2008: Determination of source depth from teleseismic *P*-wave inversion. Annual Congress of Chinese Geophysical Society and Geological Society of Taiwan, Tainan, Taiwan, May 7 - 8, 2008. (in Chinese)

Liu-Zeng, J., Z. Zhang, L. Wen, P. Tapponnier, J. Sun, X. Xing, G. Hu, Q. Xu, L. Zeng, L. Ding, C. Ji, K. W. Hudnut, and J. van der Woerd, 2009: Co-seismic ruptures of the 12 May 2008, M_s 8.0 Wenchuan earthquake, Sichuan: East-west crustal shortening on oblique, parallel thrusts along the eastern edge of Tibet. *Earth Planet. Sci. Lett.*, **286**, 355-370, doi: 10.1016/j.epsl.2009.07.017. [Link]

Mai, P. M. and G. C. Beroza, 2000: Source scaling properties from finite-fault-rupture models. *Bull. Seismol. Soc. Am.*, **90**, 604-615, doi: 10.1785/0119990126. [Link]

Nakamura, T., S. Tsuboi, Y. Kaneda, and Y. Yamanaka, 2010: Rupture process of the 2008 Wenchuan, China earthquake inferred from teleseismic waveform inversion and forward modeling of broadband seismic waves. *Tectonophysics*, **491**, 72-84, doi: 10.1016/j.tecto.2009.09.020. [Link]

Nishimura, N. and Y. Yagi, 2008: Rupture process for May 12, 2008 Sichuan earthquake. Available at http://probeinternational.org/library/wp-content/uploads/2011/11/2008-Sichuan-Earthquake.pdf.

Okal, E. A., 1992: A student's guide to teleseismic body wave amplitudes. *Seismol. Res. Lett.*, **63**, 169-180.

Pérez-Campos, X. and G. C. Beroza, 2001: An apparent mechanism dependence of radiated seismic energy. *J. Geophys. Res.*, **106**, 11127-11136, doi: 10.1029/2000JB900455. [Link]

Shen, Z. K., J. Sun, P. Zhang, Y. Wan, M. Wang, R. Bürgmann, Y. Zeng, W. Gan, H. Liao, and Q. Wang, 2009: Slip maxima at fault junctions and rupturing of barriers during the 2008 Wenchuan earthquake. *Nat. Geosci.*, **2**, 718-724, doi: 10.1038/ngeo636. [Link]

Sladen, A., 2008: Preliminary result: 05/12/2008 (M_w 7.9), East Sichuan. Available at http://www.tectonics.caltech.edu/slip_history/2008_e_sichuan/e_sichuan.html.

Vassiliou, M. S. and H. Kanamori, 1982: The energy release in earthquakes. *Bull. Seismol. Soc. Am.*, **72**, 371-387.

Wang, J. H., 2004: The seismic efficiency of the 1999 Chi-Chi, Taiwan, earthquake. *Geophys. Res. Lett.*, **31**, L10613, doi: 10.1029/2004GL019417. [Link]

Wang, W. M., L. F. Zhao, J. L., and Z. X. Yao, 2008: Rupture process of the M_s 8.0 Wenchuan earthquake of Sichuan, China. *Chin. J. Geophys.*, **51**, 1403-1410. (in Chinese)

Wen, Y. Y., K. F. Ma, and D. D. Oglesby, 2012: Variations in rupture speed, slip amplitude and slip direction during the 2008 M_w 7.9 Wenchuan Earthquake. *Geophys. J. Int.*, **190**, 379-390, doi: 10.1111/j.1365-246X.2012.05476.x. [Link]

Xu, X., X. Wen, G. Yu, G. Chen, Y. Klinger, J. Hubbard, and J. Shaw, 2009a: Coseismic reverse- and oblique-slip surface faulting generated by the 2008 M_w 7.9 Wenchuan earthquake, China. *Geology*, **37**, 515-518, doi: 10.1130/G25462A.1. [Link]

Xu, Y., K. D. Koper, O. Sufri, L. Zhu, and A. R. Hutko, 2009b: Rupture imaging of the M_w 7.9 12 May 2008 Wenchuan earthquake from back projection of teleseismic *P* waves. *Geochem. Geophys. Geosyst.*, **10**, Q04006, doi: 10.1029/2008GC002335. [Link]

Yen, Y. T. and K. F. Ma, 2011: Source-scaling relationship for *M* 4.6-8.9 earthquakes, specifically for earthquakes in the collision zone of Taiwan. *Bull. Seismol. Soc. Am.*, **101**, 464-481, doi: 10.1785/0120100046. [Link]

Yoshida, S., 1988: Waveform inversion for rupture processes of two deep earthquakes in the Izu-Bonin region. *Phys. Earth Planet. Inter.*, **52**, 85-101, doi: 10.1016/0031-9201(88)90058-1. [Link]

Zhang, Y., L. S. Xu, and Y. T. Chen, 2009: Spatio-temporal variation of the source mechanism of the 2008 great Wenchuan earthquake. *Chin. J. Geophys.*, **52**, 379-389. (in Chinese)

Zhou, Q., X. Xu, G. Yu, X. Chen, H. He, and G. Yin, 2010: Width distribution of the surface ruptures associated with the Wenchuan earthquake: Implication for the setback zone of the seismogenic faults in postquake reconstruction. *Bull. Seismol. Soc. Am.*, **100**, 2660-2668, doi: 10.1785/0120090293. [Link]

APPENDIX A

(1) Calculation of the Far-Field *P*-Waves

For a shallow earthquake, a synthetic far-field *P*-wave at a given receiver can be expressed in the following form (cf. Kanamori and Stewart 1976; Okal 1992):

$$u^P(t) = \frac{M_0}{4\pi\rho_h\alpha_h^3}\cdot\frac{g(\Delta)}{r}\cdot C^P(i_o)\cdot\Big[R^P f(t-t_p) + R^{pP}V_{pP}f(t-t_{pP}) + R^{sP}\frac{\alpha_h\cos i_h}{\beta_h\cos j_h}V_{sP}f(t-t_{sP})\Big]*Q(t)*I(t) \quad \text{(A1)}$$

where $u^P(t)$ is the synthetic far-field seismogram; M_0 is the seismic moment; α_h, β_h, and ρ_h are the *P*-wave velocity, *S*-wave velocity and density in the source area, respectively; $g(\Delta)$ denotes the geometrical spreading factor as a function of epicentral distance (Δ) and focal depth; r is the radius of the Earth (about 6371 km); R^P, R^{pP}, and R^{sP} are the radiation patterns for the *P*-, *pP*- and *sP*-waves (cf. Kanamori and Stewart 1976); V_{pP} and V_{sP} denote the reflection coefficients of the *P*- to *P*-waves and the *S*- to *P*-waves at the free surface (cf. Aki and Richards 2002); i_h and j_h are the take-off angles of the *P*- and *S*-waves just leaving the source and i_o is the incident angle of the *P*-waves to the free surface; $C^P(i_o)$ is the free surface effect at the receiver (cf. Aki and Richards 2002); $f(t)$ stands for a triangular source time function and its duration representing the source-process time; t_p, t_{pP}, and t_{sP} are the travel times for the *P*-, *pP*- and *sP*-waves, which are calculated according to a given Earth velocity model; $Q(t)$ is the attenuation filter of the earth based on Azimi's law (e.g., Yoshida 1988); $I(t)$ is the instrumental response.

After taking into account some corrections to the seismogram, we can rewrite Eq. (A1) in the following form (Lin et al. 2006).

$$\begin{aligned} u_c^P(t) &= u^P(t)\cdot 4\pi\rho_h\alpha_h^3\cdot\frac{r}{g(\Delta)}\cdot\frac{1}{C^P(i_o)} \\ &= \Big[M_0R^P f(t-t_P) + M_0R^{pP}V_{pP}f(t-t_{pP}) \\ &\quad + M_0R^{sP}\frac{\alpha_h\cos i_h}{\beta_h\cos j_h}V_{sP}f(t-t_{sP})\Big]*Q(t) \\ &= M_0R^PA_P(t) + M_0R^{pP}A_{pP}(t) + M_0R^{sP}A_{sP}(t) \end{aligned} \quad \text{(A2)}$$

$$A_P(t) = f(t-t_P)*Q(t)$$

$$A_{pP}(t) = V_{pP}f(t-t_{pP})*Q(t)$$

$$A_{sP}(t) = \frac{\alpha_h\cos i_h}{\beta_h\cos j_h}V_{sP}f(t-t_{sP})*Q(t)$$

where $u_c^P(t)$ is the corrected seismogram, not inclusive of the instrumental effect, geometrical spreading, or free surface effect. The *iasp91* velocity model (Kennett and Engdahl 1991) is used to calculate the travel time of seismic-waves as well as several parameters. The attenuation filter $Q(t)$ is calculated by Azimi's law using $t^* = 1.0$ (travel time over quality factor) for the *P*-waves (cf. Okal 1992).

The unknown parameters in Eq. (A2) are M_0, R^P, R^{pP}, and R^{sP}. Following Lin et al. (2006) and Hwang et al. (2010, 2012), Eq. (A2) can be expressed in matrix form with n data points and 3 unknown parameters (M_0R^P, M_0R^{pP}, M_0R^{sP}) as follows.

$$\begin{bmatrix} A_P(t_1) & A_{pP}(t_1) & A_{sP}(t_1) \\ A_P(t_2) & A_{pP}(t_2) & A_{sP}(t_2) \\ \cdots & \cdots & \cdots \\ A_P(t_n) & A_{pP}(t_n) & A_{sP}(t_n) \end{bmatrix} \begin{bmatrix} M_0R^P \\ M_0R^{pP} \\ M_0R^{sP} \end{bmatrix} = \begin{bmatrix} u_c^P(t_1) \\ u_c^P(t_2) \\ \cdots \\ u_c^P(t_n) \end{bmatrix} \tag{A3}$$

The parameters to be solved in Eq. (A3) are M_0R^P, M_0R^{pP}, and M_0R^{sP}, which are called the pseudo radiation patterns by Lin et al. (2006). Equation (A3) can be resolved by the standard least-squares technique. We solve the corresponding pseudo radiation pattern when giving a source duration at a fixed focal depth. Thus, by searching for a succession of source duration and focal depths, the appropriate source duration, focal depth and pseudo radiation patterns are obtained for each station by minimizing misfits between the observed and synthetic seismograms (cf. Lin et al. 2006, 2008; Hwang et al. 2010, 2012).

(2) Estimation of Radiated Seismic Energy

Following Vassiliou and Kanamori (1982), the estimated radiated seismic energy (E_S) can be written as:

$$E_S = \left[\frac{1}{15\pi\rho\alpha^5} + \frac{1}{10\pi\rho\beta^5}\right] \frac{2}{x(1-x)^2} \frac{M_0^2}{T_0^3} \tag{A4}$$

where α, β, and ρ are the P-wave velocity, S-wave velocity and density, respectively, at the source area. M_0 and T_0 are the seismic moment and source duration. Vassiliou and Kanamori (1982) used the trapezoid-type source time function with total source duration T_0 and $x = 0.2$, i.e., rise time = $xT_0 = 0.2\ T_0$, to calculate the radiated seismic energy. At $x = 0.2$, the factor $1/[x(1-x)^2]$ in Eq. (A4) is $1/0.128$. However, a triangular source time function used in this study has $x = 0.5$, making the factor $1/[x(1-x)^2]$ calculated as $1/0.125$. The two values of radiated seismic energy determined from $x = 0.2$ and $x = 0.5$ are mutually consistent.